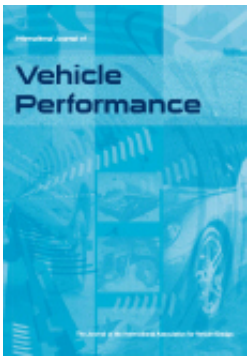


**International Journal of Vehicle Performance**

ISSN online: 1745-3208 - ISSN print: 1745-3194
https://www.inderscience.com/ijvp

# Investigation of regenerative braking for the electric mining truck based on fuzzy control

Denghao Luo, Weiwei Yang, Yilin Wang, Yijun Han, Qiang Liu, Yaodong Yang

**DOI:** 10.1504/IJVP.2023.10057687

**Article History:**

| | |
|---|---|
| Received: | 16 March 2023 |
| Last revised: | 07 June 2023 |
| Accepted: | 07 June 2023 |
| Published online: | 13 December 2023 |

# Investigation of regenerative braking for the electric mining truck based on fuzzy control

Denghao Luo, Weiwei Yang*, Yilin Wang, Yijun Han, Qiang Liu and Yaodong Yang

School of Mechanical Engineering,
University of Science and Technology Beijing,
Beijing, 100083, China
Email: 584111417@qq.com
Email: qqyangww@126.com
Email: wylg20208592@163.com
Email: hanyijun2022@163.com
Email: liuq@chinanhl.com
Email: ustbcar@ustb.edu.cn
*Corresponding author

**Abstract:** This paper proposes a braking force distribution strategy to control regenerative braking by analysing the vehicle's state so that regenerative braking does not damage the battery while recovering energy. In this paper, considering the particular characteristics of regenerative braking, a braking force distribution strategy for the front and rear axles of the vehicle is designed so that the rear axle can obtain more braking force safely. After that, a real-time optimal control strategy is proposed for regenerative braking. It uses a fuzzy control algorithm to allocate the proportion of regenerative braking by considering the battery capacity, braking intensity, and vehicle speed. The proposed strategy can recover energy while protecting the battery as much as possible. Simulation results show that the pure electric vehicle using the fuzzy control algorithm can reduce the allocation ratio of regenerative braking when the battery capacity is high, or the vehicle speed and braking intensity are high, while recovering as much energy as possible under reasonable circumstances. Therefore, the proposed regenerative braking control strategy in this paper can meet the regenerative braking requirements of pure electric vehicles.

**Keywords:** electric mining truck; regenerative braking; fuzzy control; energy management.

**Reference** to this paper should be made as follows: Luo, D., Yang, W., Wang, Y., Han, Y., Liu, Q. and Yang, Y. (2024) 'Investigation of regenerative braking for the electric mining truck based on fuzzy control', *Int. J. Vehicle Performance*, Vol. 10, No. 1, pp.73–95.

**Biographical notes:** Denghao Luo is a Master student of University of Science and Technology Beijing. His research interest is vehicle regenerative braking control strategy.

Weiwei Yang is a Lecturer of University of Science and Technology Beijing. His research interests mainly include new energy vehicle powertrain design.

Yilin Wang is a Master student of University of Science and Technology Beijing. Her research interest is vehicle regenerative braking control strategy.

Yijun Han is a Master student of University of Science and Technology Beijing. His research interest is vehicle regenerative braking control strategy.

Qiang Liu is a PhD student of University of Science and Technology Beijing. His research interest is vehicle regenerative braking control strategy.

Yaodong Yang is an Associate Professor of University of Science and Technology Beijing. His research interest is mobile equipment hydraulic transmission and control.

## 1 Introduction

After the advent of the internal combustion engine, the car gradually became the primary mode of transport. However, Dong et al. (2020) showed its reliance on fossil fuels, and the formation of pollutants after combustion increased air pollution. He et al. showed the engine has also led to a gradual increase in the share of fossil fuel consumption (He et al., 2022; Subramaniyam and Subramanian, 2020; Zhang and Cai, 2018). With the development of technology, electric vehicles are gradually coming into the public eye. Bharathidasan et al. showed purely electric vehicles could effectively reduce fossil fuels and carbon emissions, so using purely electric vehicles for transportation is the future mainstream (Bharathidasan et al., 2022; Lü et al., 2022).

Liang et al. showed that compared to traditional vehicle technology, the current pure electric vehicle technology still has some disadvantages, such as the lower energy and power density of the batteries used in electric vehicles, limited lifetime, higher costs, limited travel, and long charging times (Liang et al., 2019; Li et al., 2018; Zhang and Tong, 2022). Existing research has proposed various solutions to this set of problems.

For the problem of limited battery life in electric vehicles, thermal management is targeted at the battery to control the battery temperature to reduce battery life loss (Zhang and Tong, 2022; Wei et al., 2019). A fuzzy control algorithm is used to manage the power supply to improve the battery life (Bharathidasan et al., 2022).

For the problem of low battery energy, power density, and limited travel, it is mentioned that the energy consumed in resistance during vehicle driving accounts for 65% of the total energy consumption (Liang et al., 2019). In comparison, the energy taken up in braking is 25%. Ye et al. (2019) also mentioned the waste of braking energy in purely electric buses, so recycling the braking energy of electric vehicles is necessary. There are various ways of recovering braking energy from electric vehicles. The solution proposed is to use the drive wheel motor to recover braking energy for resistive heating to warm the vehicle in winter.

In contrast, more studies use the drive motor to recover braking energy to recharge the battery, a method known as regenerative braking. Simulation of HEVs using different regenerative braking strategies in a study verifies that regenerative braking can recover a large amount of energy (Guo et al., 2021). A study's simulation results demonstrate that regenerative braking can save up to 31% of energy under certain operating conditions (Luin et al., 2019). Rakov et al. (2020) found regenerative braking can reduce the energy consumption of a hybrid vehicle by up to 10%–16% and reduce carbon emissions by 0.2–0.5 tons/year in a city. In the study, the dynamics of the vehicle was analysed, and

the impact of regenerative braking under different braking conditions was studied (Pardhi et al., 2023).

It is clear from the literature that regenerative braking can effectively recover braking energy and increase the range of the vehicle, so research into regenerative braking is necessary for pure electric vehicles. A simulation model was used to demonstrate the specific effects of current and SOC on battery life in regenerative braking (Wu et al., 2018). Zhang et al. (2022) used simulations of various factors in the braking process to observe their effects on regenerative braking. They found that a large average deceleration speed, a large deceleration interval, and a large regenerative braking participation ratio resulted in higher energy recovery. At the same time, low temperatures would affect regenerative braking. Subramaniyam and Subramanian (2021) analysed the effects of different road surfaces on regenerative braking, and it was found that the dynamic characteristics of regenerative braking were different from those of mechanical braking and resulted in a transient decrease in vehicle braking force.

Therefore regenerative braking needs to consider a range of factors such as current, SOC, and deceleration, so it needs to develop a corresponding control. In the research, a fuzzy rule algorithm was used for HEV and a deep reinforcement learning (DRL) algorithm was used for optimisation. The feasibility of the control strategy was verified through simulation (Pukkunnen et al., 2023). Mariani et al. used an model predictive control (MPC) algorithm to control the regenerative braking and coordinate with the mechanical braking system (Li et al., 2021; Mariani et al., 2022; Wei et al., 2019; Xu et al., 2019; Ma et al., 2020). El-Bakkouri et al. used a neural network to optimise the regenerative braking controller, and the simulation verifies that the performance of this type of controller can be improved (El-Bakkouri et al., 2022; Quintero-Manríquez et al., 2021; Wang and Luo, 2022). Aksjonov et al. used a fuzzy control algorithm to specify the regenerative braking participation ratio, and the regenerative braking under fuzzy control meets the braking demand and recovers energy (Aksjonov et al., 2018; Maia et al., 2020; Xiao et al., 2017). Subramaniyam and Subramanian analysed different situations and operating conditions, and they restricted regenerative braking by using functions and rules such as ECE regulations to recover braking energy and optimise braking performance (He et al., 2022; Subramaniyam and Subramanian, 2020; Zhang and Cai, 2018).

In summary, regenerative braking has the advantages of improving vehicle mileage and increasing vehicle economy. However, the braking principle of motor braking differs significantly from conventional braking. Adding motor braking in the braking process will impact the braking performance, such as smoothness. Regenerative braking must use an electric motor, leading to a specific change in the distribution of braking force between the front and rear axles. When the battery capacity is high, the use of regenerative braking can cause damage to the battery. Therefore, the regenerative braking strategy for electric vehicles aims to set the braking force distribution between the front and rear axles. Then allocate the ratio of regenerative braking to mechanical braking so that the vehicle is as safe as possible and recovers as much energy as possible during the braking process. In the market environment that now emphasises the reduction of carbon emissions, more and more of China's mines are considering the use of pure electric mining dump trucks and one of the disadvantages that electric mining dump trucks need to address compared to fuel vehicles is the smaller range.

In contrast, mining dump trucks are basically consumed by the brake resistor in the form of heat for the current electric braking energy treatment. Hence, using regenerative braking for the current pure electric mining dump truck has a good practical significance. The control of regenerative braking is now mainly focused on the fuzzy algorithm, MPC algorithm, and reinforcement learning algorithm relying on neural network. Lu et al. (2022) used real-time wavelet transform control combined with supercapacitors to improve vehicle economy and power battery life after determining the braking force distribution strategy in a regenerative braking control strategy for a pure electric bus. It can be seen that This control strategy has good performance in urban conditions where speed changes are large and regenerative braking produces many current surges. However, it still requires the addition of a supercapacitor system to the vehicle. For mining vehicles with small speed variations and high power braking that usually needs to be maintained for a period of time, this type of control algorithm usually achieves similar performance to the fuzzy control algorithm. The advantage of fuzzy algorithms over this type of algorithm is that they are easy to use and formulate, which allows regenerative braking to be put into service more quickly for mining vehicles. In this paper, we use the TR50E mining vehicle as the object to use fuzzy control rules in a specific braking force distribution strategy to develop the regenerative braking strategy of the vehicle. Then use MATLAB simulation analysis to verify the performance of the regenerative braking strategy.

## 2 Mathematical modelling

Figure 1 shows a schematic diagram of the vehicle operation.

**Figure 1** Force diagram of the vehicle going downhill (see online version for colours)

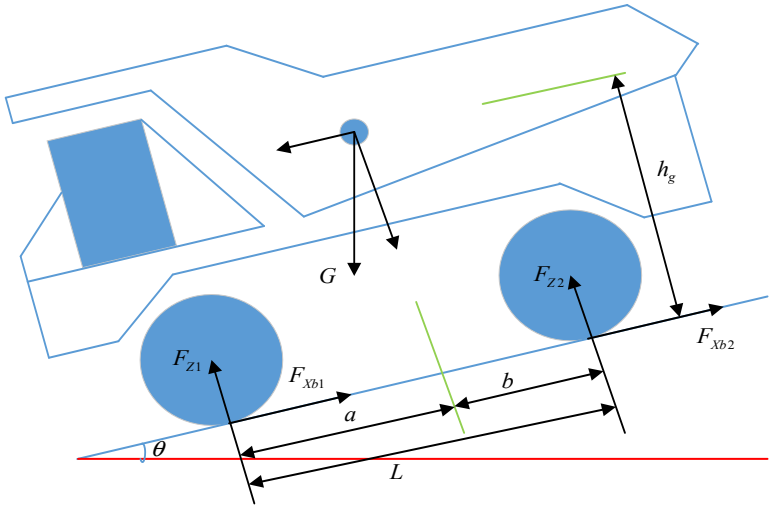


The influence of ramps should be considered in the operation of the vehicle due to the high number of ramps in the operating environment of a mining vehicle, Table 1 shows the vehicle's parameters.

**Table 1** Vehicle parameters

| *Vehicle load state* | *Distance from the centroid to the front axle a/m* | *Distance from the centroid to the rear axle b/m* | *Distance from the front axle to the rear axle L/m* | *Centroid height hg/m* | *Vehicle mass G/kg* |
|---|---|---|---|---|---|
| Empty | 2.44 | 1.62 | 4.06 | 2 | 37,000 |
| Full | 3.05 | 1.01 | | 2.55 | 82,000 |

Analysis and mathematical modelling of the vehicle's braking process: Since the mining dump truck is rear-wheel drive, the traction force on the rear axle is calculated based on the longitudinal dynamics of the vehicle.

$$\begin{cases} F = F_f + F_i + F_w + F_j \\ F = \dfrac{T_m \cdot i_T \cdot \eta_T}{R_{ro}} \\ F_f = \mu \cdot (m+M) \cdot g \cdot \cos\theta \\ F_i = (m+M) \cdot g \cdot \sin\theta \\ F_w = \dfrac{1}{2} \cdot C_D \cdot A \cdot v^2 \\ F_j = (m+M) \cdot \dfrac{dv}{dt} \end{cases} \tag{1}$$

where $F$ is the truck's traction, $F_f$ is the rolling resistance, $F_i$ is the grade resistance, $F_w$ is the air friction, $F_j$ is the acceleration resistance, $T_m$ is the motor output torque, $i_T$ is the speed ratio of two-stage planetary reducer, $\eta_T$ is the efficiency of two-stage planetary reducer, $R_{ro}$ is the drive wheel rolling radius, $\mu$ is the rolling resistance coefficient, $m$ is the no-load weight, $M$ is the load weight, $g$ is the acceleration of gravity, $\theta$ is the angle of gradient, $C_D$ is the coefficient of air resistance, $A$ is the windward area, $v$ is the driving speed.

## *2.1 Ideal braking force curve plotting*

It ensures that the front and rear wheels are held simultaneously on any road surface with a coefficient of adhesion to fully use the braking force during the braking process when the I-curve distributes the braking force making it safer in the braking process. The front and rear axle braking forces in the case of a gradient need to satisfy the following equation.

$$Fr = \sqrt{\frac{G * Ff * \cos(\theta) * L}{hg} + \left(\frac{G * \cos(\theta) * b}{2hg}\right)^2} - \left(Ff + \frac{G * \cos(\theta) * b}{2hg}\right) \tag{2}$$

where $Fr$ is the rear axle brake force, $Ff$ is the front axle brake force.

The equation for the braking force distribution curve of the vehicle, based on vehicle theory when it disregards the slope, is obtained as follows.

$$Fr = \frac{1}{2}\left[\frac{G}{hg}\sqrt{b^2 + \frac{4hgL}{G}Ff} - \left(2Ff + \frac{Gb}{hg}\right)\right] \tag{3}$$

We obtained the braking force distribution curve for a vehicle with a gradient and the braking force distribution curve without a gradient at no load and full load, as shown in Figure 2.

**Figure 2** Comparison of front and rear brake force I-curve (see online version for colours)

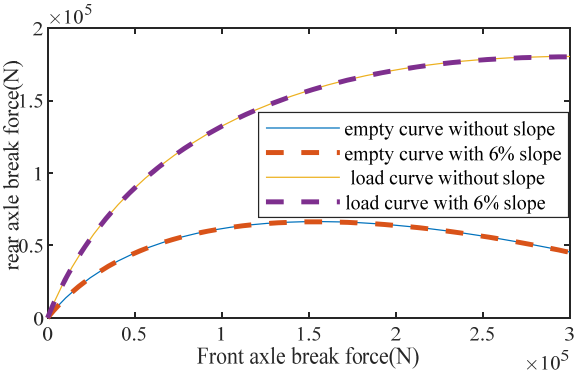


According to the operating conditions of the mining truck, the limiting slope is usually 6%, so we set the slope in the braking force distribution curve to 6% downhill. It can be seen from Figure 2 that when the vehicle is fully loaded and unloaded, the slope has minimal effect on the ideal braking force curve. Moreover, the braking force distribution curve is different between the vehicle uphill and downhill, so we ignored the slope effect in subsequent simulations for ease of use.

## 2.2 *Braking force restrictions such as ECE regulations*

When the vehicle is empty, the vehicle can be considered similar to a regular two-axle vehicle. Therefore, the braking force distribution of the vehicle is limited using the ECE regulations. According to the ECE regulations, the vehicle's front and rear wheel braking forces must satisfy the following equation for different braking intensities.

$$\begin{cases} \dfrac{b+zhg}{L} < \beta \le \dfrac{(z+0.08)(b+zhg)}{zL} (0.15 \le z \le 0.3) \\ 1-\dfrac{(z-0.02)(a-zhg)}{(0.74zL)} \le \beta \le \dfrac{(z+0.07)(b+zhg)}{(0.85zL)} (0.3 \le z \le 0.6) \\ 1-\dfrac{(z+0.07)(a-zhg)}{(0.85zL)} \le \beta \le \dfrac{(z+0.07)(b+zhg)}{0.85zL} (0.6 \le z \le 0.8) \end{cases} \tag{4}$$

where $z$ is the braking intensities, $\beta$ is the braking force distribution coefficient.

We obtained the braking force limit range of the vehicle from the ECE regulations and various parameters of the vehicle itself. At the same time, we obtained the braking force curves of the vehicle under no-load and full-load conditions by combining the front and rear braking force r curves, f curves, and I-curves of the vehicle, as shown in Figures 3(a) and 3(b).

**Figure 3** Braking force application range (see online version for colours)

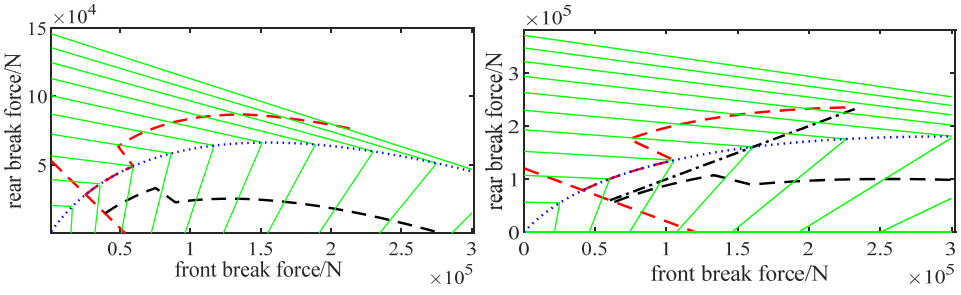


The green line in the diagram shows the r and f curves for a coefficient of adhesion of 0.1 to 1, the blue dotted line is the I-curve, and the red line is the upper limit of the rear axle braking force in the ECE regulations. When the braking strength is less than 0.15, no braking force is required, so the red line falls along the curve for a braking strength of 0.15. The black dashed line is the lower limit of the vehicle's rear axle braking force.

The black dash-dotted line in Figure 3(b) represents the braking force distribution curve at a braking force distribution factor of 0.5. As experience at full load requires the vehicle to have a braking force distribution factor of no more than 0.5, the braking force distribution at full load must be to the right of the black dash-dotted line.

## *2.3 Motor model*

The motor used in the mining truck is OD460V+1L270-2400NM. In a purely electric powertrain, the electric motor has a dual role: one is to drive the vehicle forward, and the other is to recover braking energy. In this paper, the motor ignores its complex internal dynamic characteristics. It uses a simplified motor-speed-torque model based on experimental data to obtain a peak characteristic curve, as shown in Figure 4.

**Figure 4** Motor peak characteristic curve (see online version for colours)

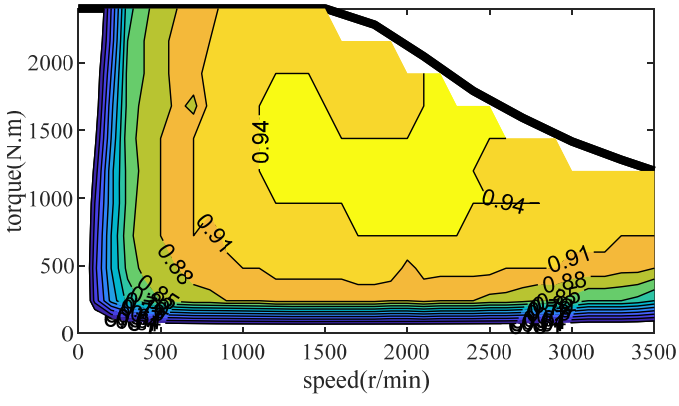


As can be seen from the diagram, the maximum speed of the motor is 3,500 r/m, while the maximum output torque is 2,400 N·m.

The expression for the relationship between motor torque and speed is as follows

$$T_m = \begin{cases} \dfrac{P_m \cdot 9{,}550}{400} & \left(n_m \le 1{,}500\ rpm\right) \\ \dfrac{P_m \cdot 9{,}550}{n_m} & \left(n_m > 1{,}500\ rpm\right) \end{cases} \tag{5}$$

where $P_m$ is the motor rated power, $n_m$ is the motor speed, $T_m$ is the motor output torque.

When taking into account the difference in motor charging and discharging efficiency, we calculated the motor power as follows

$$P_m = \begin{cases} \dfrac{T_m \cdot w_m}{\eta_m} & T_m \ge 0 \\ T_m \cdot w_m \cdot \eta_r & T_m < 0 \end{cases} \tag{6}$$

where $w_m$ is the motor output speed, $\eta_m$ is the motor discharge efficiency, $\eta_r$ is the motor charging efficiency.

## 2.4 Transmission parameters

The transmission of the electric mining truck has four gears with ratios of 8.39, 4.34, 2.27, and 1. The main reducer of the mining truck has a speed ratio of 3.15 * 5.66. After a specific time above a certain speed, the logic module will consider moving up the gears.

## 2.5 Battery model

Due to this paper's focus on regenerative braking control strategy, we ignored the transient features of the battery cell and the effect of temperature on the battery cell. The battery cell model can be simplified to a first-order approximate internal resistance model, as shown in Figure 5. Where $V_{oc}$ is the battery open circuit voltage, $R_b$ is the equivalent internal resistance of the battery, $I_b$ is the battery current, and $V_b$ is the load voltage.

**Figure 5** Diagram of the battery model

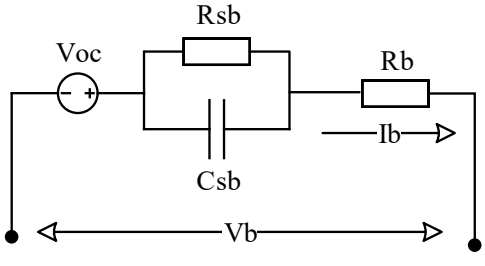


Since a battery pack comprises a certain number of battery cells connected in series and parallel, ignoring the variability between battery cells, the characteristics of a battery pack can be expressed as follows.

$$\begin{aligned} Q_b &= M_b \cdot Q_{bcell} \\ R_b &= \frac{N_b \cdot R_{bcell}}{M_b} \\ V_{oc} &= N_b \cdot V_{bcell} \end{aligned} \tag{7}$$

where $Q_b$ is the battery capacity, $Q_{bcell}$ is the individual battery capacity, $R_b$ is the internal resistance of the battery, $R_{bcell}$ is the individual cell internal resistance, $V_{bcell}$ is the individual battery voltage, $M_b$ is the number of batteries in parallel, $N_b$ is the number of batteries in series.

SOC can be calculated from the following equation

$$SOC(t) = \frac{\left(SOC_{\text{int}} \cdot Q_b - I_t\right)}{Q_b} \tag{8}$$

where $SOC_{\text{int}}$ – SOC initial value; $I_t$ – current battery current; $Q_b$ – battery capacity.

Table 2 shows the parameters of the selected battery cell.

**Table 2** Battery cell parameters

| *Rated capacity Ah* | *Nominal voltage V* | *Single-cell voltage V* | *The internal resistance of a battery cell Ω* | *Number of battery units in series* | *Number of battery units in parallel* |
|---|---|---|---|---|---|
| 627 | 577.5 | 3.5 | 0.01 | 165 | 1 |

## 3 Developing a braking strategy

The vehicle's regenerative braking strategy has two parts. Firstly the distribution of braking forces between the front and a rear axle of the vehicle determines the safety of the braking. As the electric mining truck is a rear-wheel drive vehicle, the distribution of braking force between the front and rear axles also determines to some extent recovering the amount of energy by regenerative braking.

The second is the regenerative braking force distribution strategy. This distribution strategy determines how much energy can be recovered by regenerative braking and also impacts the braking safety of the vehicle. When the braking intensity is low, the regenerative braking distribution ratio can fully use the motor for braking. In contrast, when the braking intensity is high, the regenerative braking distribution ratio should be reduced to prevent braking safety problems.

### *3.1 Braking force distribution strategy*

The following three options are now commonly used for front and rear-axle braking force distribution strategies:

1 *Braking force distribution strategy based on maximum braking energy recovery:* This braking strategy maximises the rear axle braking force to obtain maximum energy recovery, but this leads to irregular changes in the braking force curve, and the requirement for mechanical brakes leads to hysteresis and oscillation when braking, which affects the braking performance of the vehicle. In this model, the

braking force curve is the maximum value of the red line in Figure 3, and use the rear axle brakes only when the braking intensity is low.

2 *Braking force distribution strategy based on I-curve:* This strategy distributes the braking force along the I-curve as possible to achieve better performance. However, it reduces the motor involvement in braking and results in less energy recovery from the motor. The braking force curve is the blue dotted line of Figure 3 in this model

3 *Braking force control strategy based on rule:* This strategy uses the motor for braking at low braking intensities and distributes the braking force along the I-curve when the braking intensity is high. In this model, the rear axle works first when the braking intensity is low, and the front axle provides the remaining braking force when the rear axle reaches 28,668 N. The braking force is distributed along the I-curve in Figure 3 when the braking intensity is greater than 0.15.

### *3.2 Regenerative brake distribution strategy*

In analysing the braking strategy for this dump truck, the rear axle always uses the motor to participate in braking first. Mechanical braking provides the remaining braking force as the braking force distribution strategy for the rear axle. So when the battery SOC is high, the motor braking will cause more significant damage to the battery. At the same time, in the braking process, some sudden situations will require emergency braking. When the braking intensity suddenly reaches the emergency braking demand value, the motor braking needs to be withdrawn in time while the mechanical braking needs to take part in time. At this time, there is a high possibility of safety problems, so the fuzzy algorithm can optimise the braking strategy.

#### *3.2.1 Regenerative braking fuzzy controller design*

We used the fuzzy toolbox in MATLAB to implement the design of the fuzzy control strategy in this section and to design a three-input, one-output fuzzy controller with Mamdani inference selected for fuzzy inference. The control inputs are braking intensity, battery, and driving speed. The output is the motor braking distribution coefficient. The control inputs and output selected suitable affiliation functions in the controller. Figure 6 shows the fuzzy control input interface.

**Figure 6** Fuzzy control input interface (see online version for colours)

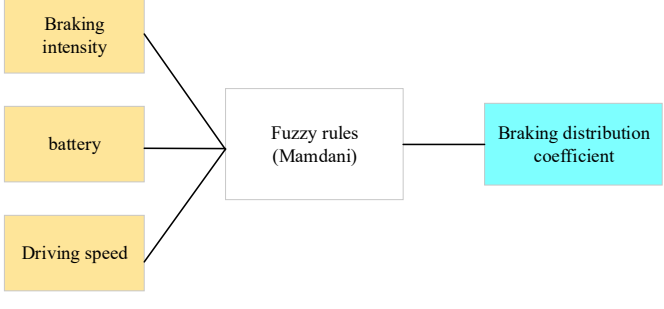

### *3.2.1.1 Braking strength fuzzing*

The magnitude of braking intensity represents the driver's braking intention, which usually varies between 0 and 1 depending on the braking demand. Therefore, set [0, 1] to the braking intensity domain, the quantisation level is 3, with three different levels of braking demand {small (S), medium (M), and large (L)}. The affiliation function of braking intensity is chosen as a triangle and trapezoid. Figure 7 shows the degree of braking strength.

**Figure 7** Degree of braking strength function (see online version for colours)

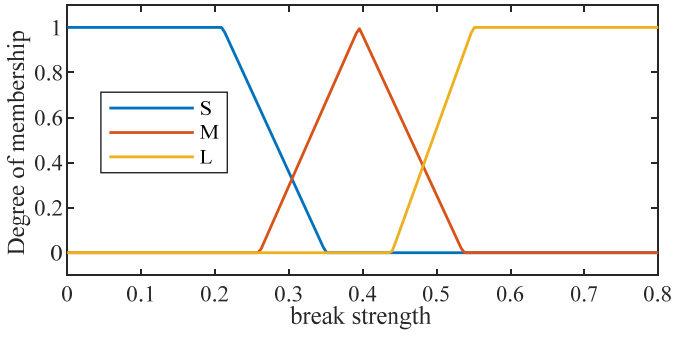


When the braking intensity is 'S', the driver's braking demand is not strong, so the motor can be fully involved in braking. When the braking intensity is 'M', the braking demand is moderate. The motor can be braking when it is considered safe to do so. As the braking intensity increases, the proportion of motor involvement in braking will be reduced. When the braking intensity is 'L', the vehicle is in an emergency braking state, and the motor is no longer involved in braking.

### *3.2.1.2 Battery SOC fuzzing*

The influence of the battery SOC value on energy recovery lies mainly in the safety of battery use. The domain of the battery SOC value is [0, 1], the quantisation level is 5, and the fuzzy language variables are used to measure the battery power with {VS (very small), S (small), M (medium), L (large), VL (very large)}. The triangle and trapezoid are chosen for the degree of SOC value, and Figure 8 shows the degree of SOC.

When the battery SOC value is less than 90%, the energy recovery system charges the battery. When the SOC is 'VS' and 'S', the battery charge is very low, so the motor braking ratio can be taken as the maximum. When the SOC is 'M', the battery charge is medium, and the energy recovery system recovers energy appropriately. When the SOC is 'L', the battery charge is large, and the energy recovery systems begin to reduce the percentage of energy recovered. When SOC is 'VL', means the SOC value is greater than 90%, and the motor recovers a small amount of energy to protect the battery.

### *3.2.1.3 Speed fuzzing*

Dump trucks usually travel in the speed range of 0–30 km/h, so the domain of vehicle speed is set as [0, 30]. The quantisation level is three, and the fuzzy language of vehicle speed is taken as {L (low), M (medium), H (high)}. Figure 9 shows the degree of the

speed. Less energy is recovered at lower vehicle speeds, and more energy is recovered at higher vehicle speeds.

**Figure 8** The degree of the SOC function (see online version for colours)

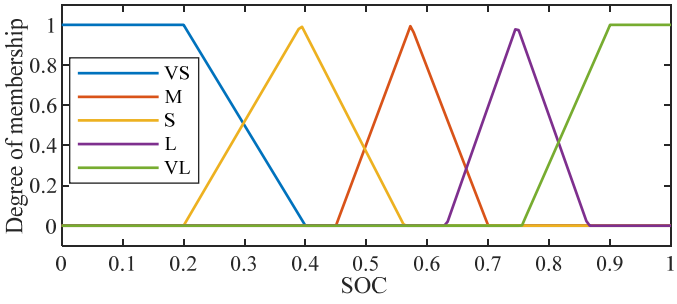


**Figure 9** The degree of the speed function (see online version for colours)

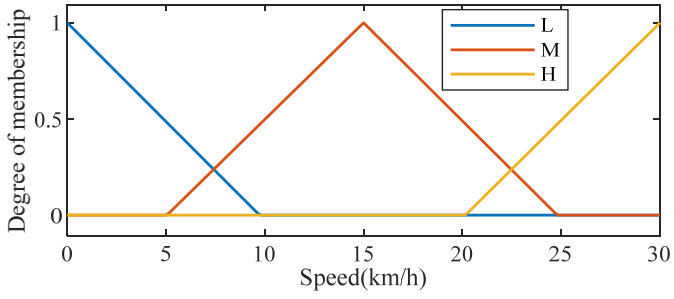


**Figure 10** The degree of the distribution coefficient function (see online version for colours)

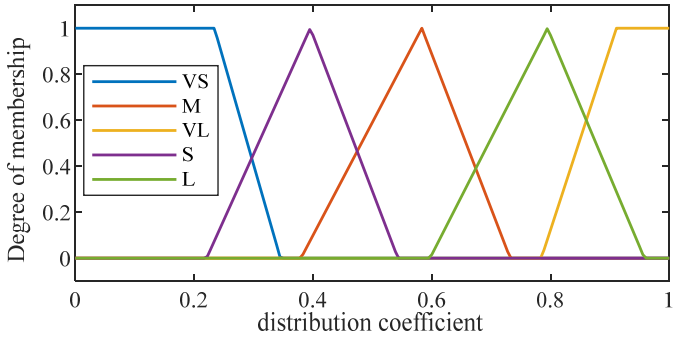


### *3.2.1.4 Fuzzing motor brake distribution coefficient*

The motor braking proportional coefficient represents the proportion of the braking force of the front axle motor. The larger the distribution coefficient means, the higher the proportion of the braking force involved in the motor, the domain of the distribution coefficient is taken as [0, 1], and the quantisation level is 5. The fuzzy language takes {VS (very small), S (small), M (medium), L (large), VL (very large)} to indicate the

degree of motor involvement. The affiliation function is chosen as a triangle and trapezoid. Figure 10 shows the degree of the distribution coefficient.

### *3.2.1.5 Fuzzy rules*

The energy recovery fuzzy control rule should consider the safety of braking and the energy recovery capability of the vehicle and integrate the influence of the three inputs on energy recovery to reason about the optimal proportional output value for click braking. This paper uses a three-input, one-output fuzzy controller, and the rule expression is expressed in the form of 'if Z and V and SOC, then K'.

When the braking intensity and speed are 'M', and the SOC value is 'L', the vehicle speed and the braking intensity are moderate, and the battery is not enough. So the braking situation is safer now, so the motor can be allocated a larger proportion of braking. Therefore, the distribution factor K is a value in the L range. Similar to this experience, this paper obtained 45 fuzzy control rules. Table 3 shows the specific fuzzy control rules.

**Table 3** Fuzzy control strategy table

| *k* | | *SOC* | | | | |
|---|---|---|---|---|---|---|
| | | *VS* | *S* | *M* | *L* | *VL* |
| V(Z = S) | L | VL | M | M | S | VS |
| | M | VL | L | L | M | VS |
| | H | VL | VL | VL | L | VS |
| V(Z = M) | L | S | S | S | S | VS |
| | M | L | L | M | M | VS |
| | H | VL | VL | L | M | VS |
| V(Z = L) | L | VS | VS | VS | VS | VS |
| | M | VS | VS | VS | VS | VS |
| | H | VS | VS | VS | VS | VS |

Figure 11 shows the results of the fuzzy control. As expected from the theoretical analysis, the proportionality coefficient of motor involvement in braking increases with decreasing braking intensity, SOC, and increases with increasing vehicle speed.

**Figure 11** Fuzzy control results (see online version for colours)

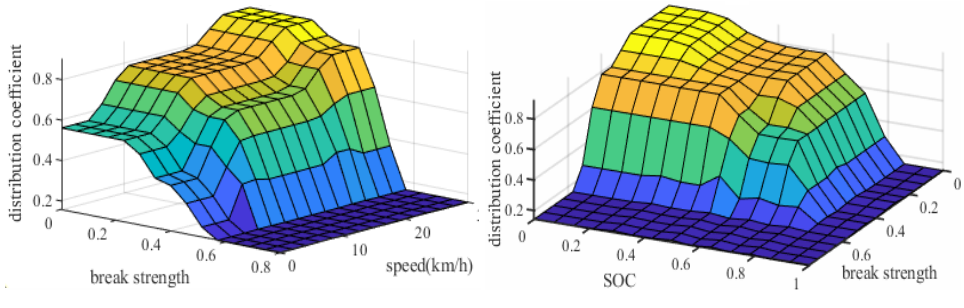


(a) (b)

### 3.3 Braking strategy evaluation indicators

The indicators used to evaluate regenerative braking performance are battery SOC and energy recovery efficiency.

Braking distance is the distance travelled during the vehicle's braking, and the battery SOC represents the battery's capacity. The energy recovery efficiency is the ratio of the energy recovered to the energy storage system during braking to the total energy required to brake the vehicle during driving.

$$\varphi = \frac{E_1}{E_2} \tag{9}$$

$E_1$ is the energy collected by the battery, and $E_2$ is the total energy required for braking.

## 4 Simulation research

### 4.1 The general architecture of the simulation model

Based on the MATLAB/Simulink r2021b simulation platform, the main components are the braking energy recovery strategy, the battery module, the driver module, the transmission module, and the vehicle module. In this paper, a forward simulation modelling structure is used, which allows the vehicle to be driven and braked according to the required operating conditions through the driver's control role, which is closer to actual vehicle driving conditions.

The braking strategy module uses four systems to represent the braking force distribution curves under different braking strategies and braking intensities to obtain the braking forces for the front and rear axles under the corresponding braking strategies. After the braking forces are output, the results are obtained, which can be optimised using the fuzzy control module.

Inputting the braking intensity, SOC value and vehicle speed into the fuzzy control module. Then it outputs the braking force distribution coefficient $k$ to distribute the electric motor power. The fuzzy control module is not involved in the braking force strategy simulation and then participates in the simulation verification when the braking force strategy is determined.

### 4.2 Analysis of simulation results

The primary working environment of the mining truck is poor road conditions, so the road surface adhesion coefficient is set to 0.6, and the speed of the mining truck is required not to exceed 30 km/h when it is fully loaded. At the same time, the mining truck's operation road conditions have a particular slope and different mass, so the operating environment is simulated with the working conditions in Figure 12. The working conditions in Figure 12 are obtained from the actual vehicle with sensors running in the mine and then processed, where

a is the speed of the vehicle in the mine

b is the loading of the vehicle

c is the slope of the vehicle during driving

d is the braking intensity in the driving condition.

**Figure 12** Vehicle simulation conditions (see online version for colours)

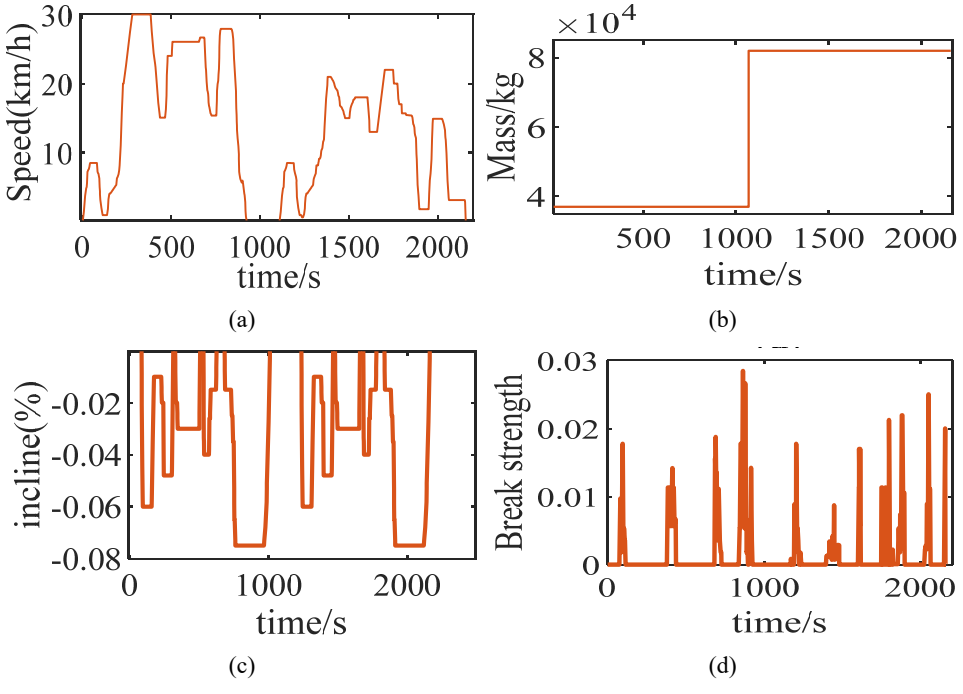


### *4.2.1 Simulation of front and rear axle braking force*

Firstly, the simulation used the maximum braking energy recovery strategy. Figure 13 shows the simulation results. In Figure 13(a) shows that the braking strategy can maintain excellent speed tracking during braking, and it can be seen from Figure 13(c) that a high energy recovery efficiency can be maintained throughout the braking process, at this time it can be seen in the braking force distribution diagram Figure 13(b) that the main focus is on motor braking, and the energy that is not recovered is mainly consumed in the driving resistance and other components.

In the empty state, the motor brakes throughout the working conditions. At full-load state, the force required for braking is greater, and at the same time, due to the higher speed of the vehicle, the motor speed is higher, resulting in less motor braking force. Therefore, a mechanical brake is added at high speed and with high braking intensity. When the speed drops and the motor brake can meet the braking force demand, the mechanical brake exits the braking process.

After that, the simulation used the braking strategy based on I-curve. Figure 14 shows the simulation results. In Figure 14(c) shows that the efficiency of the best braking performance. The difference between the braking strategies in energy recovery is greater than the recovery efficiency of the maximum braking energy recovery strategy. Because when using the best braking performance braking strategy, the front and rear axle braking

forces are distributed according to the I-curve. There is always energy consumed in the mechanical braking part. In terms of SOC, the optimal braking strategy has a lower SOC than the maximum braking energy recovery strategy, indicating that less braking energy is recovered. Regarding braking force distribution, the front axle braking force is higher with the optimal braking performance strategy than with the maximum braking energy.

**Figure 13** The maximum braking energy recovery strategy (see online version for colours)

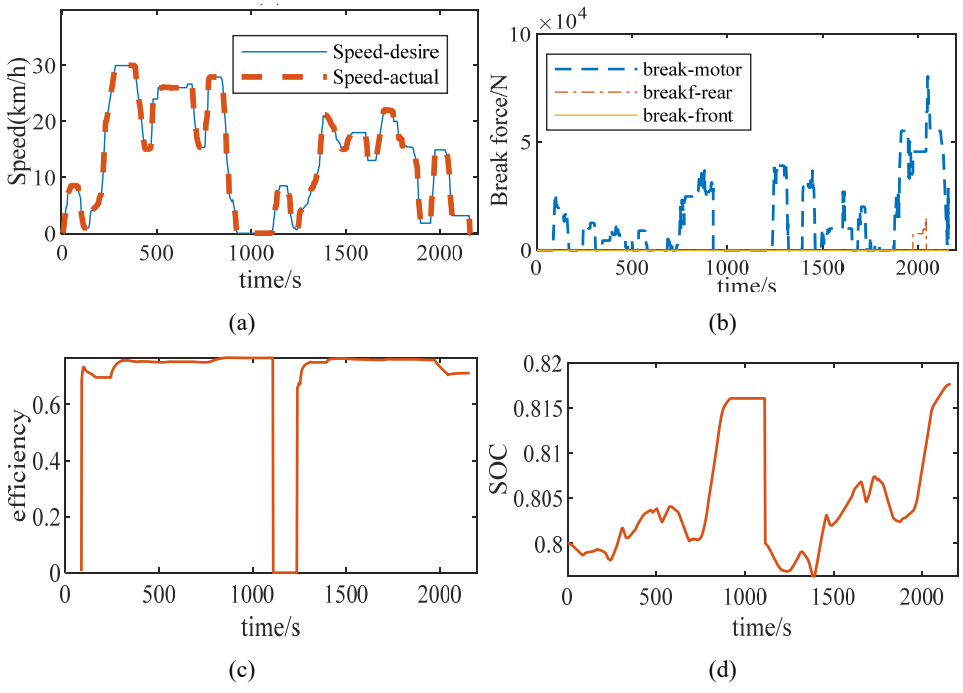


Figure 15 shows the simulation results. The braking strategy can have an energy recovery efficiency close to the maximum braking energy recovery strategy when in an empty state. In contrast, the energy recovery efficiency decreases when the braking intensity is higher, but it can also have a high level. In terms of SOC, the optimised braking strategy is similar to the maximum braking energy recovery strategy.

**Figure 14** The braking strategy based on I-curve (see online version for colours)

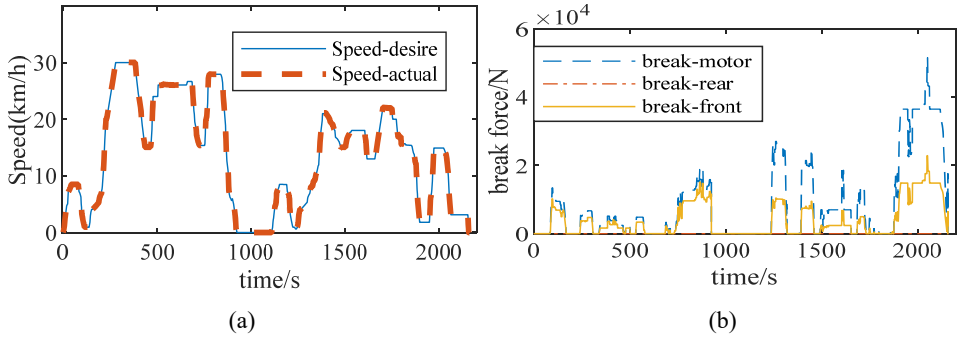

**Figure 14** The braking strategy based on I-curve (continued) (see online version for colours)

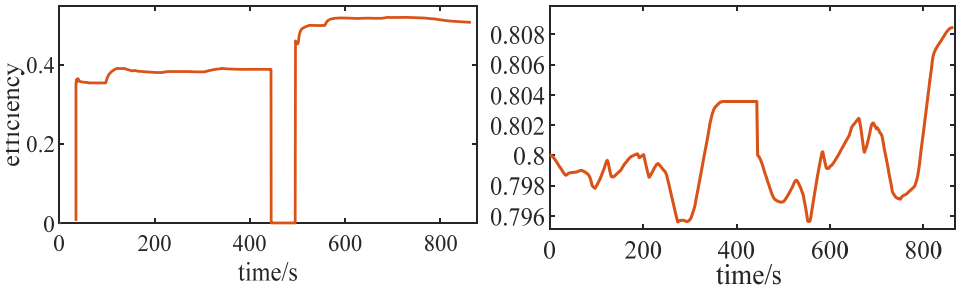


**Figure 15** The braking strategy based on rule (see online version for colours)

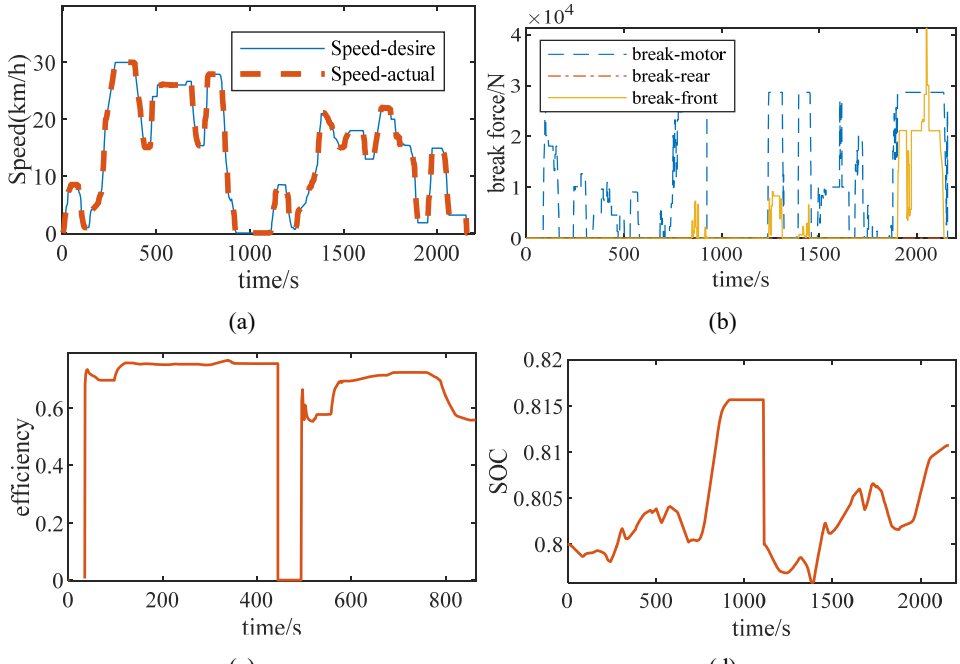


According to the simulation results and braking force curves of the three braking strategies, it can be concluded that the comprehensive consideration braking strategy can make the braking force change more smoothly while recovering the braking energy as much as possible. In contrast, the maximum energy recovery strategy can obtain higher braking energy. However, when the speed is higher at full load or the braking intensity is greater, it is still possible to use the motor brake, leading to driving safety problems. So the integrated considering braking strategy is used as the basis for the braking force distribution between the front and rear axles in the fuzzy control simulation.

**Figure 16** Simulated vehicle speed and slope (see online version for colours)

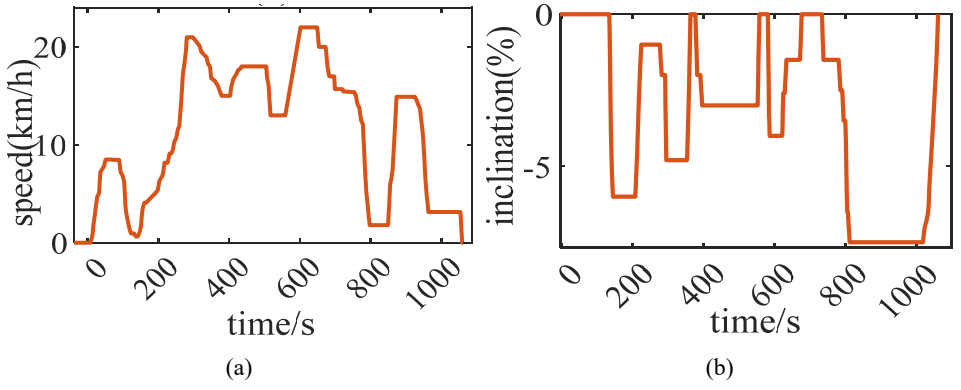


**Figure 17** Simulation results for SOC = 0.8 (see online version for colours)

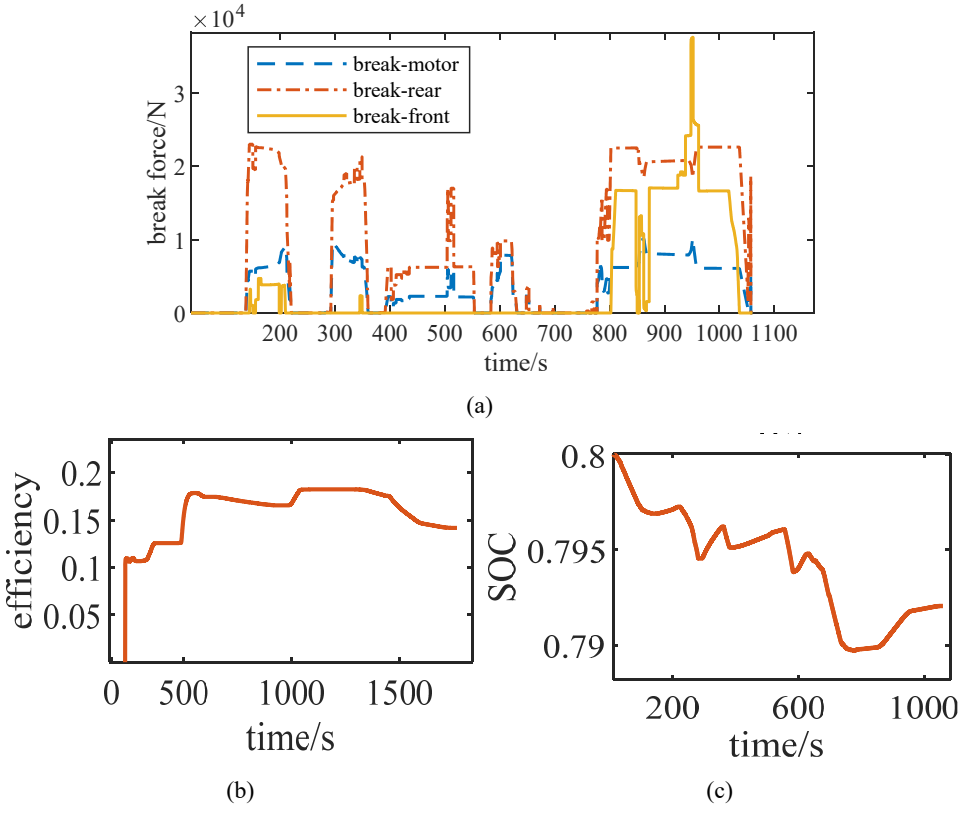


### *4.2.2 Simulation of the fuzzy control algorithm*

As can be seen from the previous braking simulation, the braking force distribution at the rear axle always follows the regenerative braking strategy, where the motor brakes are the main part, and the remaining braking force is made up of the mechanical brakes. On the

one hand, when the battery capacity is high, continuing to use regenerative braking to recharge the battery will cause damage to the battery. On the other hand, when the braking intensity is high, and the vehicle speed is fast, it is not safe to continue to use the motor brake, and the motor brake should be made to exit in time. Therefore, the paper applies the fuzzy algorithm to the regenerative braking force distribution.

**Figure 18** Simulation results for SOC = 0.5 (see online version for colours)

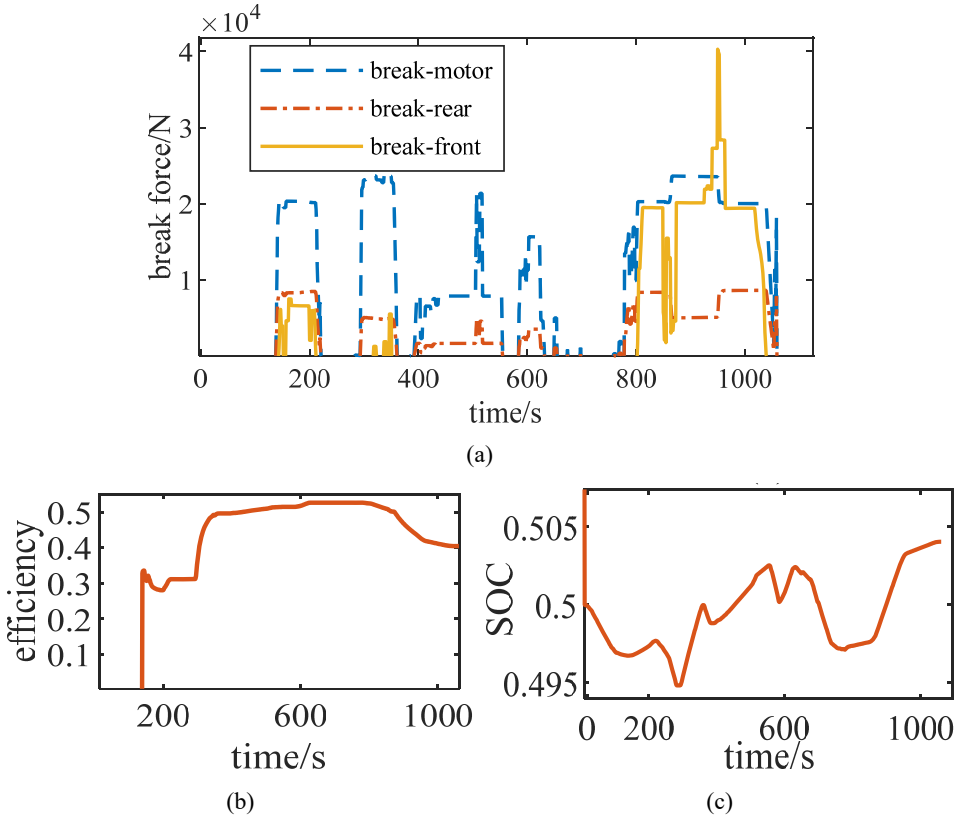


Because of the significant difference between the forces on the vehicle at empty and full load, the fuzzy control algorithm must be able to meet the full load situation when it is not. The vehicle at full load needs to pay more attention to safety. Therefore, in the simulation of the fuzzy algorithm only for full load simulation, the full-load state uses the same operating conditions as shown in Figure 16, and the vehicle braking strategy uses a comprehensive optimisation of the braking force control strategy. The battery capacity was set to 0.8, 0.5, and 0.3 for the simulation after the fuzzy algorithm was used because the battery capacity greatly influenced the fuzzy algorithm.

Figure 17 shows the simulation results for the battery capacity of 0.8. In Figure 17(c) shows that under the fuzzy algorithm control, when the battery capacity is 80%, the battery is unsuitable for regenerative braking, regenerative braking accounts for a smaller proportion of the total braking force. The energy recovery efficiency is lower, which keeps the SOC below 80%, which is in line with the expectation of fuzzy control and can effectively protect the battery.

**Figure 19** Simulation results for SOC = 0.3 (see online version for colours)

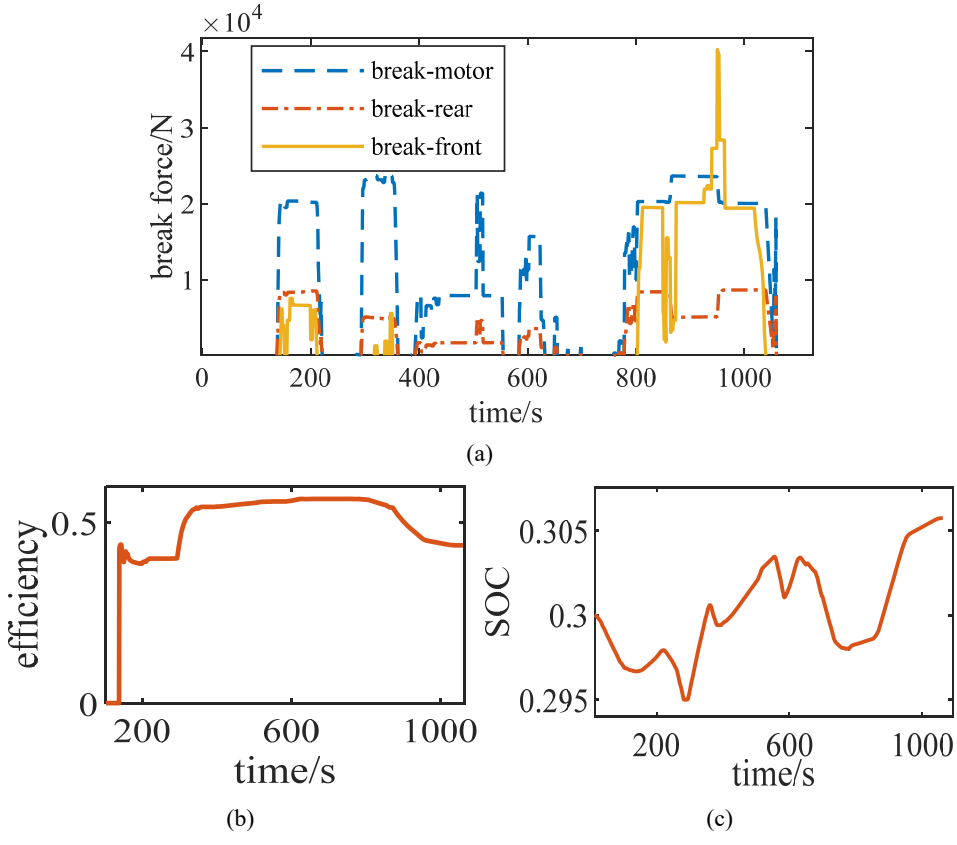


Figure 18 shows the fuzzy simulation results when the SOC is 0.5. When the SOC is 0.5, the battery is in a state suitable for charging, so the percentage of the motor regenerative braking force in the total braking force increases, and at around 900 seconds, when there is a sudden large change in the braking force demand, the motor regenerative braking gradually decreases. From Figure 18(c), it can be seen that the battery capacity is medium when the battery can be effectively recharged on downhill slopes as expected by the fuzzy control.

Figure 19 shows the fuzzy simulation results when the SOC is 0.3. From Figure 19(b), it can be seen that the vehicle under the control of the fuzzy algorithm can achieve a braking energy recovery rate of 56.5%. In Figure 19(a) shows that the fuzzy control still reduces the regenerative braking force of the motor at higher vehicle speeds and higher braking intensities in the lower battery SOC value. At the same time, due to the SOC value of 0.3, the fuzzy algorithm increases the proportion of the motor involved in braking, and from Figure 19(c), it can be seen that more energy is recovered compared to when SOC = 0.5, as expected from fuzzy control.

Combined with the above simulation content, the braking force control strategy proposed in this paper is feasible. The fuzzy control algorithm is used to optimise the braking force control strategy, which can effectively balance the safety, battery life, and energy recovery efficiency during the vehicle's braking process.

## 5 Conclusions

This paper investigates the regenerative braking of an electric mining truck. First a rule-based braking force distribution strategy for front and rear axle is designed. Simulation results reveal that it can make the braking force of the rear axle as large as possible during braking while ensuring safety. The strategy allows the truck to gain more energy through regenerative braking safely compared to the I-curve. Second, a composite brake control strategy is designed. It uses a fuzzy control algorithm to analyse the vehicle's battery capacity, speed and braking intensity to output the corresponding regenerative braking force ratio. Simulation results demonstrate that the proposed control strategy can recover as much braking energy as possible while protecting the battery. However, there are certain shortcomings when using the fuzzy algorithm. In the future work, the optimised control strategy will be studied, for instance, MPC and DRL.

## Acknowledgements

This work was supported by the Guangdong Basic and Applied Basic Research Foundation (No. 2021A1515110195), Central University Basic Research Fund of China (No. FRF-TP-20-054A1), and Shunde Graduate School of University of Science and Technology Beijing.

## References

Aksjonov, A., Vodovozov, V., Augsburg, K. et al. (2018) 'Design of regenerative anti-lock braking system controller for 4 in-wheel-motor drive electric vehicle with road surface estimation', *International Journal of Automotive Technology*, Vol. 19, pp.727–742.

Bharathidasan, M., Indragandhi, V., Suresh, V. et al. (2022) 'A review on electric vehicle: technologies, energy trading, and cyber security', *Energy Reports*, Vol. 8, pp.9662–9685.

Dong, H., Fu, J., Zhao, Z et al. (2020) 'A comparative study on the energy flow of a conventional gasoline-powered vehicle and a new dual clutch parallel-series plug-in hybrid electric vehicle under NEDC', *Energy Conversion and Management*, Vol. 218, p.113019.

El-Bakkouri, J., Ouadi, H. and Saad, A. (2022) 'Adaptive neuro fuzzy inference system based controller for electric vehicle's hybrid ABS braking', *IFAC-PapersOnLine*, Vol. 55, No. 12, pp.371–376.

Guo, H., Zhang, J., Geng, W. et al. (2021) 'Research on regenerative braking strategies for hybrid electric vehicle by co-simulation model', *International Journal of Vehicle Performance*, Vol. 7, Nos. 3–4, pp.188–206.

He, Q., Yang, Y., Luo, C. et al. (2022) 'Energy recovery strategy optimization of dual-motor drive electric vehicle based on braking safety and efficient recovery', *Energy*, Vol. 248, p.123543.

Li, L., Ping, X., Shi, J. et al. (2021) 'Energy recovery strategy for regenerative braking system of intelligent four-wheel independent drive electric vehicles', *IET Intelligent Transport Systems*, Vol. 15, No. 1, pp.119–131.

Li, N., Zhang, J., Zhang, S. et al. (2018) 'The influence of accessory energy consumption on evaluation method of braking energy recovery contribution rate', *Energy Conversion and Management*, Vol. 166, pp.545–555.

Liang, J., Walker, P.D., Ruan, J. et al. (2019) 'Gearshift and brake distribution control for regenerative braking in electric vehicles with dual clutch transmission', *Mechanism and Machine Theory*, Vol. 133, pp.1–22.

Lu, Q., Zhou, W. and Zheng, Y. (2022) 'Regenerative braking control strategy with real-time wavelet transform for composite energy buses', *Machines*, Vol. 10, No. 8, p.673.

Lü, X., Li, S., He, X. et al. (2022) 'Hybrid electric vehicles: a review of energy management strategies based on model predictive control', *Journal of Energy Storage*, Vol. 56, p.106112.

Luin, B., Petelin, S. and Al-Mansour, F. (2019) 'Microsimulation of electric vehicle energy consumption', *Energy*, Vol. 174, pp.24–32.

Ma, H., Chu, L., Guo, J. et al. (2020) 'Cooperative adaptive cruise control strategy optimization for electric vehicles based on SA-PSO with model predictive control', *IEEE Access*, Vol. 8, pp.225745–225756.

Maia, R., Mendes, J., Araújo, R. et al. (2020) 'Regenerative braking system modeling by fuzzy Q-learning', *Engineering Applications of Artificial Intelligence*, Vol. 93, p.103712.

Mariani, V., Rizzo, G., Tiano, F.A. et al. (2022) 'A model predictive control scheme for regenerative braking in vehicles with hybridized architectures via aftermarket kits', *Control Engineering Practice*, Vol. 123, p.105142.

Pardhi, S., Deshmukh, A. and Ajrouche, H. (2023) 'Modelling of detailed vehicle dynamics and quantitative impact of electric motor placement on regenerative braking', *International Journal of Vehicle Performance*, Vol. 9, No. 1, pp.16–40.

Pukkunnen, E.B., Joseph, N.M., Jos, B.M. et al. (2023) 'Performance investigation and energy optimisation in hybrid electric vehicle model using reinforcement learning and fuzzy controller', *International Journal of Vehicle Performance*, Vol. 9, No. 1, pp.73–90.

Quintero-Manríquez, E., Sanchez, E.N., Antonio-Toledo, M.E. et al. (2021) 'Neural control of an induction motor with regenerative braking as electric vehicle architecture', *Engineering Applications of Artificial Intelligence*, Vol. 104, p.104275.

Rakov, V., Kapustin, A. and Danilov, I. (2020) 'Study of braking energy recovery impact on cost-efficiency and environmental safety of vehicle', *Transportation Research Procedia*, Vol. 50, pp.559–565.

Subramaniyam, K.V. and Subramanian, S.C. (2020) 'Wheel slip regulation of electrified heavy road vehicles using regenerative braking', *IFAC-PapersOnLine*, Vol. 53, No. 1, pp.422–427.

Subramaniyam, K.V. and Subramanian, S.C. (2021) 'Impact of regenerative braking torque blend-out characteristics on electrified heavy road vehicle braking performance', *Vehicle System Dynamics*, Vol. 59, No. 2, pp.269–294.

Wang, Q. and Luo, Y. (2022) 'Research on a new power distribution control strategy of hybrid energy storage system for hybrid electric vehicles based on the subtractive clustering and adaptive fuzzy neural network', *Cluster Computing*, Vol. 25, pp.4413–4422.

Wei, C., Hofman, T., Caarls, E.I. et al. (2019) 'Zone model predictive control for battery thermal management including battery aging and brake energy recovery in electrified powertrains', *IFAC-PapersOnLine*, Vol. 52, No. 5, pp.303–308.

Wu, J., Wang, X., Li, L. et al. (2018) 'Hierarchical control strategy with battery aging consideration for hybrid electric vehicle regenerative braking control', *Energy*, Vol. 145, pp.301–312.

Xiao, B., Lu, H., Wang, H. et al. (2017) 'Enhanced regenerative braking strategies for electric vehicles: dynamic performance and potential analysis', *Energies*, Vol. 10, p.1875.

Xu, W., Chen, H., Zhao, H. et al. (2019) 'Torque optimization control for electric vehicles with four in-wheel motors equipped with regenerative braking system', *Mechatronics*, Vol. 57, pp.95–108.

Ye, L., Liang, C., Liu, Y. et al. (2019) 'Performance analysis and test of a novel eddy-current braking & heating system for electric bus', *Energy Conversion and Management*, Vol. 183, pp.440–449.

Zhang, H., Chen, D., Zhang, H. et al. (2022) 'Research on the influence factors of brake regenerative energy of pure electric vehicles based on the CLTC', *Energy Reports*, Vol. 8, Supplement 14, pp.85–93.

Zhang, L. and Cai, X. (2018) 'Control strategy of regenerative braking system in electric vehicles', *Energy Procedia*, Vol. 152, pp.496–501.

Zhang, Y. and Tong, L. (2022) 'Regenerative braking-based hierarchical model predictive cabin thermal management for battery life extension of autonomous electric vehicles', *Journal of Energy Storage*, Vol. 52, Part A, p.104662.